

Accelerated Design of Optimized Implantable Antennas for Medical Telemetry

Asimina Kiourti, *Student Member, IEEE*, and Konstantina S. Nikita, *Senior Member, IEEE*

Abstract—We modify our latest reported methodology for implantable antenna design, in an attempt to further accelerate the design while achieving optimized resonance characteristics. Design is performed inside a small-sized single- or multi-layer tissue box for the Single-Layer Tissue Model (SLTM) and the Multi-Layer Tissue Model (MLTM) variations, respectively. Given a specific medical application scenario, the idea is to take into account the dielectric loading of the surrounding tissues and exterior air on the antenna, while using an adequately small tissue model to speed-up simulations. Effectiveness of the methodology is assessed for antenna design aimed at intra-cranial pressure (ICP) monitoring and cardiac pacemaker applications. The MLTM variation provides more accurate results than the SLTM at the expense of being slightly more complex and slow.

Index Terms—Implantable antenna, Medical Device Radiocommunications Service (MedRadio) band, optimization.

I. INTRODUCTION

IMPLANTABLE medical devices (IMDs) are nowadays attracting significant scientific interest for medical diagnosis and treatment [1]–[3]. A key component of an IMD is the implantable antenna which is integrated into the IMD to accommodate its telemetry with exterior medical equipment. The Medical Device Radiocommunications Service (MedRadio) band (401–406 MHz) is most commonly used for medical implant telemetry [4]. Implantable antenna design is highly demanding, with one of the major challenges being the fast design of antennas with optimized resonance characteristics within the medical application in hand [5].

Since implantable antennas will operate inside human tissue rather than inside free-space, their design must take into account the proper dielectric loading. It has, thus, been suggested to perform implantable antenna design while in the center of a 100 mm-edge cube filled with tissue-simulating dielectric material [6], [7]. However, further implantation of the designed antenna inside the intended implantation site will detune its resonance frequency, as attributed to the variation in dielectric loading by the surrounding tissues and exterior air. To account for this detuning, it has lately been proposed to further place the designed antenna inside a canonical model of the intended implantation site and automatically refine its

design through Quasi-Newton optimization [7]. Nevertheless, the technique is relatively time-consuming, since it involves antenna design within two different tissue models (cube and canonical tissue model), which exhibit increased dimensions.

In this study, the aforementioned methodology is modified in an attempt to further accelerate the design of implantable antennas with optimized resonance characteristics. The modified methodology takes into account the dielectric loading of the surrounding tissues and exterior air on the antenna, and optimizes its design within a small-sized single- (Single-Layer Tissue Model (SLTM) variation) or multi-layer (Multi-Layer Tissue Model (MLTM) variation) tissue box. Effectiveness is assessed for antenna design aimed at intra-cranial pressure (ICP) monitors and cardiac pacemakers.

II. PROPOSED METHODOLOGY

A. Antenna Model and Motivation Behind the Methodology

A parametric model of a MedRadio implantable antenna is considered (Fig. 1), which has been experimentally validated by the authors [7], [8]. The antenna consists of a ground plane (radius, R , of 6 mm) and two vertically stacked patches (radius of 5 mm) printed on Rogers RO 3210 substrates (thickness of 0.6 mm). A Rogers RO 3210 superstrate (thickness of 0.6 mm) covers the structure to prevent contact between the metal and human tissues. Meanders of variable lengths (L_i , $i = 1-5$, $1'-6'$) are inserted into the patches to assist in antenna miniaturization while allowing for tuning refinement. Meandering modifies the current path onto the radiating patches into a serpentine shape (Fig. 1(b) and (c)), thus increasing the effective length of the current flow, and reducing the antenna resonance frequency for given physical dimensions. A shorting pin (S : $x = 1$ mm, $y = -4$ mm) connects the ground plane with the lower patch, while a 50 Ohm coaxial cable excites both patches (F : $x = 0$ mm, $y = 4$ mm).

Three exposure scenarios are considered: (a) antenna in free-space (Fig. 2(a)), (b) antenna in the center of a 10^6 mm³ cube filled with skin-emulating liquid at 402 MHz [1] (Fig. 2(b)), and (c) antenna at the edge of the same 10^6 mm³ cube (Fig. 2(c)). Meander lengths are tuned for skin-implantation [7], and numerical (Ansoft HFSS [9]) as well as experimental results of the reflection coefficient frequency response are shown in Fig. 2(a)–(c), respectively. Dielectric loading of the antenna by the surrounding tissues and exterior air is found to significantly affect its resonance performance. When the

Manuscript received October 14, 2012; revised December 12, 2012.

The authors are with the School of Electrical and Computer Engineering, National Technical University of Athens, Athens 15780, Greece (e-mail: akiourti@biosim.ntua.gr; knikita@ece.ntua.gr).

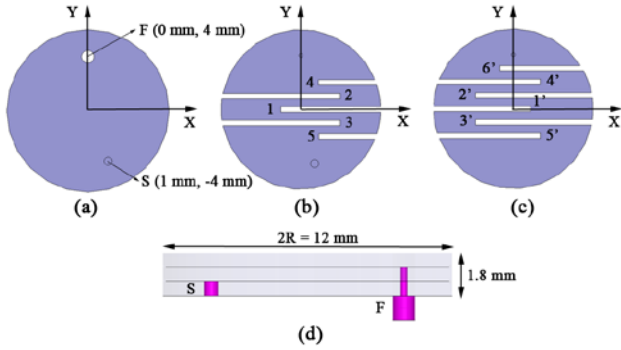


Fig. 1. Parametric implantable antenna model: (a) ground plane, (b) lower patch, (c) upper patch, and (d) side view.

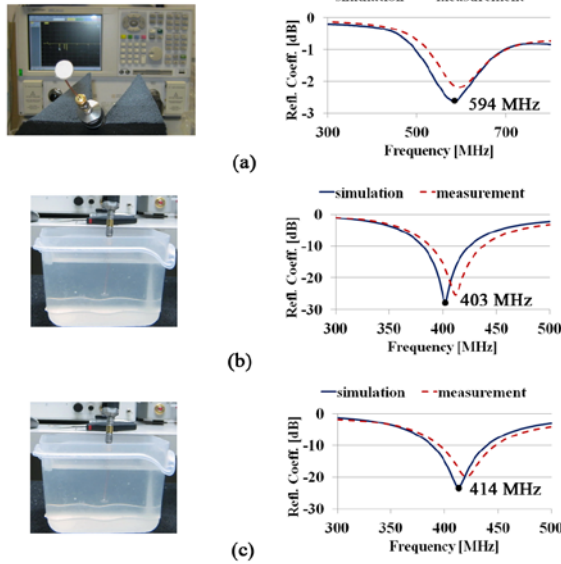


Fig. 2. Exposure scenarios and reflection coefficient frequency response: (a) antenna in free-space, (b) antenna in the center of a skin-cube, and (c) antenna at the edge of a skin-cube.

antenna is surrounded by skin-tissue (Scenario (b)), then the desired resonance is achieved in the MedRadio band. However, radiation in free-space (Scenario (a)) or at the edge of the skin-emulating cube (Scenario (c)) decreases the effective dielectric loading on the antenna (permittivity of free-space is much lower than that of skin-tissue) and increases the exhibited resonance frequency. Therefore, if the combined dielectric loading effect of the surrounding tissues and exterior air is appropriately taken into account, then antenna design can significantly be accelerated and optimized.

B. Variation I: Single-Layer Tissue Model (SLTM)

Implantable antenna design using the SLTM variation is performed within a small tissue box which accounts for the dielectric loading effect of the exterior air. The flow chart is shown in Fig. 3.

Meander lengths (L_i , $i = 1-5$, $1'-6'$) are initialized to random values, and the antenna is placed at a distance d under the outer surface of the tissue-simulating box shown in the inset of Fig. 3 (SLTM). The distance d corresponds to the actual air-to-antenna separation distance for the desired medical application (implantation depth). The tissue-simulating box extends by $R + 4$ mm in the X and Y directions

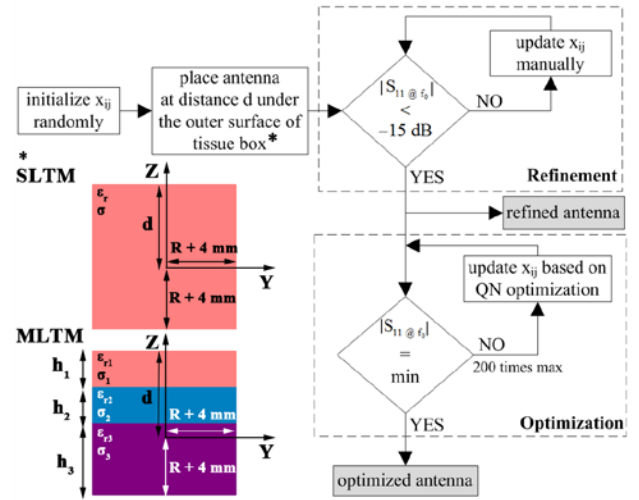


Fig. 3. Flow chart of the SLTM and MLTM variations.

(R is the maximum dimension of the antenna in the positive Y axis), and simulates the dielectric properties (permittivity, ϵ_r , and conductivity, σ) of the intended implantation tissue. Further enlargement of the box insignificantly affects the resonance performance of the antenna.

In the first step (“Refinement”), approximate antenna design is performed. Meander lengths are manually updated in an iterative way, until the magnitude of the reflection coefficient ($|S_{11}|$) at the desired operation frequency (f_0) satisfies

$$|S_{11@f_0}| < -15 \text{ dB} . \quad (1)$$

In the second step (“Optimization”), antenna design is optimized. Meander lengths are initialized to the values of the refinement step and are considered as dimensions in the Quasi-Newton optimization solution space [10]. The optimization process terminates when

$$|S_{11@f_0}| = \min , \quad (2)$$

or when the number of iterations exceeds 200.

C. Variation II: Multi-Layer Tissue Model (MLTM)

Implantable antenna design using the MLTM variation is performed within a small tissue box which accounts for the dielectric loading effect of the exterior air and the heterogeneity of the surrounding tissue environment. The MLTM follows the same flow chart as that of the SLTM (Fig. 3). The only difference is that simulations are now carried out inside a multi-layer tissue box (Fig. 3, inset).

The multi-layer tissue box includes multiple dielectric layers of adequate thickness, which correspond to the tissue layers of the intended implantation site. Three tissue layers of thicknesses t_1, t_2 and t_3 are shown in the inset of Fig. 3, which have been found to provide highly precise results. The antenna is implanted inside the proper tissue layer, as indicated in the inset of Fig. 3. The distance d along the Z axis corresponds to the actual air-to-antenna separation distance within the

desired medical application (implantation depth). The tissue-simulating box extends by $R + 4$ mm in the X and Y directions (R is the maximum dimension of the antenna in the positive Y axis), and each of the layers simulates the dielectric properties (permittivity, ϵ_r , and conductivity, σ) of the corresponding tissues. Same as for the SLTM, further enlargement of the box insignificantly affects the antenna resonance performance.

III. RESULTS

The SLTM and MLTM variations are applied to design optimized antennas for implantation inside the skin tissue of the human head (ICP monitors) and the muscle tissue of the human trunk (cardiac pacemakers). Finite Element (FE) simulations are carried out in Ansoft HFSS [9]. The FE solver automatically meshes the geometry in an iterative way. The mesh is perturbed by 30% between each pass, and the meshing procedure stops when the maximum change in the magnitude of the reflection coefficient between two consecutive passes is less than 0.02 or when the number of passes exceeds 10. Radiation boundaries are set $\lambda_0/4$ ($\lambda_0 = c / f_0$, where $f_0 = 403$ MHz) away from the models in order to extend radiation far and guarantee stability of the numerical simulations. A Quasi-Newton optimizer is integrated into the platform. Meander lengths (L_i , $i = 1-5$, $1'-6'$) of the parametric antenna model (Fig. 1) vary within the range [0 mm, 9.5 mm], in minimum and maximum steps of 0.1 and 0.5 mm, respectively.

A. Antenna Design for ICP Monitors

The parametric antenna model ($R = 6$ mm, Fig. 1) is implanted at a distance of $d = 3$ mm under the outer surface of the tissue boxes, which corresponds to the actual average implantation depth inside the human scalp. The single-layer tissue box of the SLTM is modeled to mimic skin tissue properties at 403 MHz ($\epsilon_r = 46.72$, $\sigma = 0.69$ S/m) (Fig. 3, inset), whereas the multi-layer tissue box of the MLTM is modeled to mimic skin ($h_1 = 5$ mm), bone ($h_2 = 5$ mm) and grey matter ($h_3 = 3$ mm) tissue properties at 403 MHz ($\epsilon_{r1} = 46.72$, $\sigma_1 = 0.69$ S/m, $\epsilon_{r2} = 13.14$, $\sigma_2 = 0.09$ S/m, $\epsilon_{r3} = 57.38$, $\sigma_3 = 0.74$) (Fig. 3, inset) [11].

Optimized values of the meander lengths are given in Table I (“Skin / Head”). The reflection coefficient frequency responses of the SLTM-optimized antenna implanted inside the single-layer tissue box (solid line), as well as inside the skin tissue of a three-layer spherical head model (dotted line) (Fig. 4(a)) are shown in Fig. 4(b). The corresponding MLTM numerical results are shown in Fig. 4(c). The head model consists of skin (thickness of 5 mm), bone (thickness of 5 mm) and brain tissues [7]. Implantation inside a canonical tissue model of the intended implantation site rather than inside the miniature single- (SLTM) or multi- (MLTM) layer tissue boxes results in minor frequency detunings of 2 MHz and 0 MHz, respectively.

B. Antenna Design for Cardiac Pacemakers

The parametric antenna model ($R = 6$ mm, Fig. 1) is implanted at a distance of $d = 20$ mm under the outer surface

	Skin / Head		Muscle / Trunk	
	SLTM	MLTM	SLTM	MLTM
L_1	6.496	6.296	7.396	5.496
L_2	8.936	9.036	7.736	7.636
L_3	7.936	8.936	7.636	9.336
L_4	3.165	1.265	1.865	2.665
L_5	2.365	1.665	2.465	3.865
$L_{1'}$	9.496	9.596	9.796	8.696
$L_{2'}$	8.936	9.036	9.036	9.136
$L_{3'}$	8.036	9.036	9.436	8.936
$L_{4'}$	8.265	8.365	5.965	7.565
$L_{5'}$	7.365	7.565	8.365	8.665
$L_{6'}$	7.442	7.442	5.842	6.142

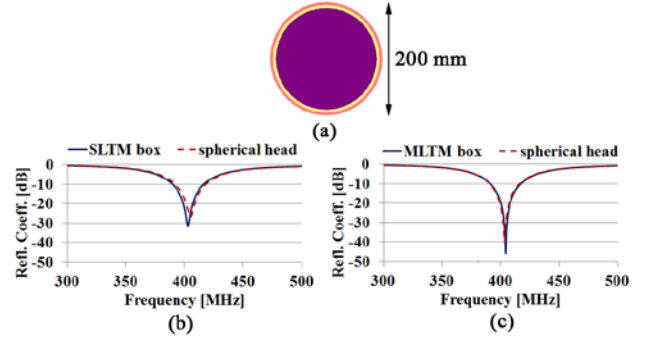


Fig. 4. Antenna design for ICP monitors: (a) spherical head model, (b) performance of the SLTM, and (c) performance of the MLTM.

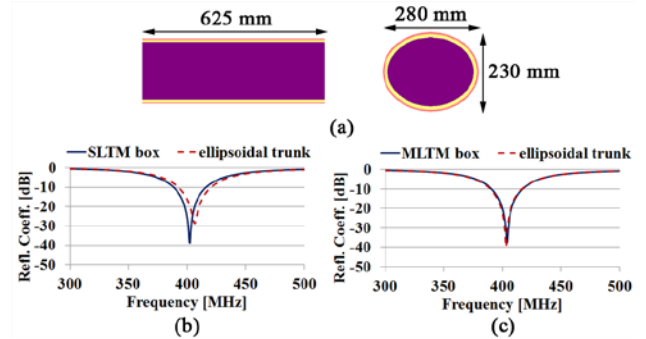


Fig. 5. Antenna design for cardiac pacemakers: (a) ellipsoidal trunk, (b) performance of the SLTM, and (c) performance of the MLTM.

of the tissue boxes, which corresponds to the actual average implantation depth inside the human muscle for cardiac pacemaker applications. The single-layer tissue box of the SLTM is modeled to mimic muscle tissue properties at 403 MHz ($\epsilon_r = 57.10$, $\sigma = 0.80$ S/m) (Fig. 3, inset), whereas the multi-layer tissue box of the MLTM is modeled to mimic skin ($h_1 = 5$ mm), fat ($h_2 = 10$ mm) and muscle ($h_3 = 12$ mm) tissue properties at 403 MHz ($\epsilon_{r1} = 46.72$, $\sigma_1 = 0.69$ S/m, $\epsilon_{r2} = 5.58$, $\sigma_2 = 0.04$ S/m, $\epsilon_{r3} = 57.10$, $\sigma_3 = 0.80$ S/m) (Fig. 3, inset) [11].

Optimized values of the meander lengths are given in Table I (“Muscle / Trunk”). The reflection coefficient frequency responses of the SLTM-optimized antenna implanted inside the single-layer tissue box (solid line), as well as inside the muscle tissue of an ellipsoidal trunk model (dotted line) (Fig. 5(a)) are shown in Fig. 5(b). The corresponding MLTM numerical results are shown in Fig. 5(c). The trunk model consists of skin (thickness of 5 mm), fat (thickness of 10 mm) and muscle tissues [12]. Implantation inside a canonical tissue

TABLE II
COMPARATIVE ANALYSIS OF THE SLTM, THE MLTM, AND THE LATEST REPORTED METHODOLOGY FOR IMPLANTABLE ANTENNA DESIGN [7]

	[7]	SLTM	MLTM
tissue models	model 1: 100 mm–edge skin cube model 2: 100 mm–radius spherical head	13 * 20 * 20 mm ³ skin box	13 * 20 * 20 mm ³ three–layer box (skin, fat, muscle)
time per simulation	~ 2 min in model 1 ~ 6.50 min in model 2	~ 1.5 min	~ 1.75 min
overall design time	~ 465 min	~ 113 sec	~ 131 sec
detuning in spherical head	0 MHz	2 MHz	0 MHz

model of the intended implantation site rather than inside the miniature single– (SLTM) or multi– (MLTM) layer tissue boxes results in minor frequency detunings of 4 MHz and 0 MHz, respectively.

C. Discussion

Numerical results verify the suitability of the SLTM and MLTM variations for accelerated and optimized design of implantable antennas, regardless of the medical application in hand (i.e. intended implantation tissue and implantation depth). Since the MLTM accounts for the dielectric loading effect of both the exterior air and the surrounding heterogeneous tissue environment, it is found to be more accurate. Regarding the head– and trunk–implantation example applications under study, zero frequency detunings were computed for the MLTM as compared to the 2 MHz and 4 MHz frequency detunings of the SLTM, respectively. On the other hand, the SLTM single–layer tissue box is easier to model and can be meshed in larger tetrahedra, which render the SLTM variation slightly faster to implement.

As compared to the latest reported methodology for implantable antenna design [7], the SLTM and MLTM variations further accelerate the design. Numerical results inside small–sized tissue boxes are found to be almost identical to those inside canonical models of the intended implantation site, thus, rendering design directly into the latter unnecessary and inadequately slow. Effectiveness has been assessed within canonical models of the intended implantation sites, in an attempt to simplify and speed–up simulations. As already demonstrated by the authors, canonical tissue models are equally suitable to anatomical ones for assessing the performance of implantable antennas [7], [13].

Performance of the SLTM, the MLTM, and the latest reported methodology for implantable antenna design [7] is compared in Table II. Indicative results are given for antenna design aimed at ICP monitoring ($R = 6$ mm), carried out in a PC with a 2.83 GHz processor and 3.25 GB of installed RAM.

IV. CONCLUSION

In this study, we modified our latest reported methodology for implantable antenna design, in an attempt to further accelerate the design of optimized implantable antennas. Novelty lies in selecting a small–sized single– (SLTM) or multi–layer (MLTM) tissue box, and strategically placing the antenna inside it for design purposes. The aim is to incorporate the dielectric loading of the exterior air (SLTM) or the dielectric loading of both the exterior air and the surrounding heterogeneous tissue environment (MLTM). Design of

implantable antennas for ICP monitoring and cardiac pacemaker applications demonstrated that, though slightly more complex and slow, the MLTM provides more accurate results than the SLTM. However, both the SLTM and the MLTM occur to be faster than the latest reported methodology for implantable antenna design [7], while achieving optimized resonance characteristics for the medical application in hand.

ACKNOWLEDGMENT

The work of A.K. was supported by the IEEE Microwave Theory and Techniques Society Graduate Fellowship for Medical Applications. The authors would like to thank Dr. C. Fernandes and Dr. J. Costa for providing the facilities of Instituto de Telecomunicações, Instituto Superior Técnico, Lisbon, Portugal, and helping with the prototype fabrication.

REFERENCES

- [1] T. Karacolak, A. Z. Hood, and E. Topsakal, “Design of a dual–band implantable antenna and development of skin mimicking gels for continuous glucose monitoring,” *IEEE Trans. Microw. Theory Tech.*, vol. 56, pp. 1001–1008, Apr. 2008.
- [2] R. Warty, M.–R. Tofighi, U. Kawoos, and A. Rosen, “Characterization of implantable antennas for intracranial pressure monitoring: reflection by and transmission through a scalp phantom,” *IEEE Trans. Microw. Theory Tech.*, vol. 56, pp. 2366–2376, Oct. 2008.
- [3] T. Karacolak, R. Cooper, J. Butler, S. Fisher, and E. Topsakal, “In vivo verification of implantable antennas using rats as model animals,” *IEEE Antennas Wireless Propag. Lett.*, vol. 9, pp. 334–337, 2010.
- [4] Federal Communications Commission [Online] <http://www.fcc.gov>
- [5] A. Kiourti and K.S. Nikita, “A review of implantable patch antennas for biomedical telemetry: challenges and solutions,” *IEEE Antennas Propag. Mag.*, vol. 54, pp. 210–228, Jun. 2012.
- [6] A. Kiourti, M. Christopoulou, and K. S. Nikita, “Performance of a novel miniature antenna implanted in the human head for wireless biotelemetry,” in *Proc. IEEE Int. Symp. Antennas Propag.*, Spokane, WA, 2011, pp. 392–395.
- [7] A. Kiourti and K.S. Nikita, “Miniature scalp–implantable antennas for telemetry in the MICS and ISM bands: design, safety considerations and link budget analysis,” *IEEE Trans. Antennas Propag.*, vol. 60, pp. 3568–3575, Aug. 2012.
- [8] A. Kiourti, J.R. Costa, C.A. Fernandes, A.G. Santiago, and K.S. Nikita, “Miniature Implantable Antennas for Biomedical Telemetry: from Simulation to Realization,” *IEEE Trans. Biomed. Eng.*, vol. 59, no. 11, pp. 3140–3147, Nov. 2012.
- [9] Ansoft High Frequency Structure Simulator (HFSS), Ver. 11, Ansoft Corporation, 2008.
- [10] W. Sun and Y.–X. Yuan, *Optimization Theory and Methods*. New York: Springer, 2006, ch. 5, Ed.
- [11] C. Gabriel, S. Gabriel, and E. Corthout, “The dielectric properties of biological tissues,” *Phys. Med. Biol.*, vol. 41, pp. 2231–2293, 1996.
- [12] K. Shiba, M. Nukaya, T. Tsuji and K. Koshiji, “Analysis of current density and specific absorption rate in biological tissue surrounding transcatheter transformer for an artificial heart,” *IEEE Trans. Biomed. Eng.*, vol. 55, pp. 205–213, Jan. 2008.
- [13] A. Kiourti and K.S. Nikita, “Numerical assessment of the performance of a scalp–implantable antenna: effects of head anatomy and dielectric parameters,” *Wiley Bioelectromagnetics* (to appear).